Environ Monit Assess (2024) 196:136
https://doi.org/10.1007/s10661-023-12149-x

RESEARCH

A novel removal of Ni^{2+} ions from water solutions using dispersive solid-phase extraction method with nano Fe_3O_4/chitosan-acrylamide hydrogel

Morteza Parsayi Arvand · Ali Moghimi · Narges Salehi

Received: 14 April 2023 / Accepted: 18 November 2023 / Published online: 11 January 2024

Abstract The effluent release containing heavy metals as Ni^{2+} ions has drastic risks to both the natural environment and human health. In this research, the nano Fe_3O_4/chitosan-acrylamide hydrogel was prepared as a novel nano sorbent for dispersive solid-phase extraction of Ni^{2+} ions and applied to the water sample solution. The pH, amount and type of elution solvent, the extraction time, etc. were optimized to improve the efficiency of the proposed method. Analytical parameters such as concentration factor and relative standard deviation (%) were achieved as 33.3 and 1.8%, respectively. The capacity in equilibrium sorption was calculated at 22.54 mg g^{-1}. Furthermore, to estimate the adsorption mode, Freundlich, Langmuir, and Temkin models were fitted with experimental isotherm data. Besides, to check the basic process of the metal adsorption mechanism, pseudo-first-order, pseudo-second-order, and Roginsky-Zeldovich models were investigated and the results were fitted with the pseudo-second-order model. The value of change in entropy ($\triangle$S) obtained is −65.24 (J(mol K)$^{-1}$). Negative values of change in enthalpy, $\triangle$H in (kJ mol^{-1}) is −24.45 (kJ mol^{-1}) which indicates both physical and chemical adsorptions involved in the process of adsorption. Finally, the nano Fe_3O_4/chitosan-acrylamide hydrogel exhibited high performance to remove the Ni^{2+} ions from water sample solution.

Keywords Dispersive solid phase extraction · Removal · Magnetic sorbent · Ni^{2+} ions · Chitosan · Acrylamide

Introduction

At low concentrations, nickel (Ni) acts as a micronutrient and a toxin in marine systems and freshwater. At high levels of this element, it can bind to the cell membrane and prevent the transfer process through the cell wall (Izatt et al., 1985). For the normal metabolism of many living organisms, it requires about 40 ng mL^{-1} of Ni (Gomes-Gomes et al., 1995). Also, Ni compounds have many industrial uses and so increase the pollutants in the environment (Ghazanfar et al., 2021). Therefore, new methods for preconcentration, determination, and selective removal of trace amount of Ni in various samples, such as industrial, medicinal, and environmental water samples, have been considered.

In the past years, different methods similar to reverse osmosis, membrane adsorption, ion-exchange,

M. P. Arvand
Department of Chemistry, Islamshahr Branch, Islamic Azad University, Islamshahr, Iran

A. Moghimi (✉) · N. Salehi
Department of Chemistry, Faculty of Pharmaceutical Chemistry, Tehran Medical Sciences, Islamic Azad University, Tehran, Iran
e-mail: alimoghimi@iauvaramin.ac.ir; kamran9537@yahoo.com; ali.moghimi@iaups.ac.ir

and cloud point extraction were applied for the removal of heavy metals from wastewater (Fu & Wang, 2011). But these techniques have several limits and difficulties, such as low performance and sludge production (Jiang et al., 2015). The adsorption method was often proposed to remove heavy metals from wastewater due to its simplicity, high efficiency, low cost, low toxicity, and easy scale-up (Joshi & Srivastava, 2019; Khan et al., 2011; Rasoulzadeh et al., 2021). By using magnetic nanomaterial particles as adsorbents in solid phase extraction (SPE), which is actually called magnetic solid phase extraction (MSPE), due to the high specific surface area of nanomaterials and the use of magnets without centrifugation or sample purification, the adsorption capacity increases and it becomes easier to separate the analyte from the sample (Bagheri et al., 2011; Wierucka & Biziuk, 2014).

After cellulose, chitosan is the second natural polysaccharide obtained from deacetylation of chitin. Chitin is found in crustaceans, arthropods, mollusks, and the cell walls of some fungi (Sadeghi-Kiakhani et al., 2019). Chitosan is an inexpensive biosorbent that has been effective in the removal of heavy metals due to its biocompatible, biodegradable, several functional groups such as hydroxyl, amino, and Estamido group (Rahangdale and Kumar 2018). Due to the low acid stability, poor recyclability, and mechanical properties of chitosan, functional group grafting is usually used to improve its stability and adsorption (Miretzky & Cirelli, 2009 ; Mourya & Inamdar, 2008 ; Salehi et al., 2022; Varma et al., 2004).

Recently, acrylamide-grafted chitosan was used by Al-Karawi et al., and the results showed that increasing the functional groups on chitosan increased the adsorption capacity of copper (II) in chitosan (Al-Karawi et al., 2011). Among different techniques, spectrometric methods, especially flame and graphite furnace atomic absorption spectrometry (AAS), are commonly used for the determination of Ni (Boudreau & Cooper, 1989; Kvitek et al., 1982).

The aim of the current research is to synthesize a new nanomagnetic adsorbent, which for the first time is used to preconcentrate Ni^{2+} ions, high extraction efficiency and then determine it by flame atomic absorption spectroscopy (FAAS). First, the adsorbent was synthesized by modifying chitosan with Fe_3O_4 nanoparticles and acrylamide to increase the functional groups of chitosan and improve its properties. On the other hand, the magnetic particles caused easy separation without the need for centrifugation or purification of the sample. Then, the magnetic nano sorbent was characterized by FT-IR, XRD, and SEM. After optimizing the effective parameters on Ni^{2+} ions adsorption using the suggested method, the experimental data were fitted on the isotherm and adsorption kinetics models. Also, thermodynamic parameters for the adsorption of Ni^{2+} on nano Fe_3O_4/chitosan-acrylamide hydrogel were obtained. Finally, results showed that this method was simple, efficient, strategic, economical, and successfully applied in the removal of Ni^{2+} ions in water and wastewater samples.

Materials and methods

Reagents

Chitosan (deacetylation rate more than 90% and 99% purity), acrylamide (99% purity), and Ni(II) chloride ($NiCl_2{\cdot}2H_2O$, 98% purity) were provided by Fluka Co. Potassium chlorate ($KClO_3$, 99.55% purity), sulfuric acid (H_2SO_4(with purity more than 97%, nitric acid (HNO_3) with purity more than 63%, hydrochloric acid with purity more than 37%, sodium hydroxide with purity more than 98%, and ethanol ((C_2H_6O(with purity more than 99.9%) were acquired from Fluka, Germany. All other chemical agents were in analytical grade and applied without further purification. Ni(II) stock solution (1000 mg L^{-1}) was prepared using deionized water.

Instruments

The infrared spectroscopy was recorded by FTIR spectrometer (FTIR, Thermo, AVATAR, MA, USA). The patterns of X-ray diffraction (XRD) obtained were performed on a Philips PW-1800 diffractometer apparatus (Cu Kα radiation). The SEM images of scanning electron microscopy were taken with the microscope of scanning electron (Philips, model EM-3200). The concentration of Ni^{2+} ions was analyzed by the PG-990 flame spectrophotometer and atomic absorption of graphite furnace spectrometer (PG, England). The choice of the FAAS method was due to the availability and cheapness of this method. To compare the results in real samples, we also

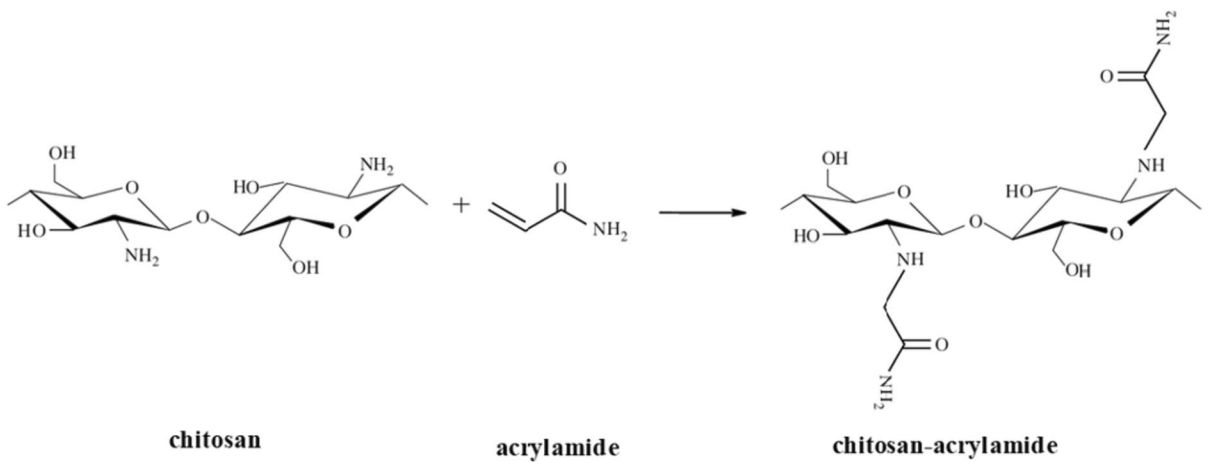

Scheme 1 Synthesis of chitosan-acrylamide

measured the samples by the graphite furnace spectrometer. The aqueous samples were separated by centrifugation (Hettich, Universal 320). An ultrasonic apparatus (UP400S, Hielscher) was used for sonication. The pH measurements of solutions were done by a pH meter (PB-11, Sartorius).

Synthesis of nano iron oxide

Separately, 2.5 g of $FeCl_2$ and 5 g of $FeCl_3$ were dissolved in 50 mL of distilled water. A flask was used to combine the two solutions. One side of the mixture was kept continually under nitrogen gas, while the other side received 50 mL of 3 M NaOH, which was added and vigorously stirred for 1 h at 60 °C. It was then rinsed in distilled water to get the pH level down to 7, and finally, it was dried in a 70 °C oven.

Hydrogel preparation

The 20 mL of distilled water was used to dissolve 5 mL of acrylic acid monomer, and then 0.1 g of chitosan is added. The mixture was then well stirred for 4 h before being strained. A 5 g of acrylamide was dissolved in 20 mL of distilled water before adding acrylic acid/chitosan (filtered solution). The monomer solution was added to 0.1 g of nano-iron oxide dissolved in 10 mL of water in a small beaker and stirred with a glass stirrer, and then 0.2 g of ammonium persulfate as an initiator and 0.05 g of N,N′-methylenebisacrylamide as a cross-linker were combined in the same beaker and placed at a temperature of 70 °C under nitrogen gas, where polymerization took place. The polymer was then dried in a vacuum oven at a temperature of 60 °C. Scheme 1 shows the synthesis of chitosan-acrylamide. In fact, Fe_3O_4/chitosan-acrylamide hydrogel is synthesized via Schiff's base formation between amino groups in chitosan and acrylamide.

Removal of Ni^{2+} ions from aqueous solutions

The adsorption behavior of Fe_3O_4/chitosan-acrylamide hydrogel towards the Ni^{2+} ions was investigated in detail. In fact, the result of pH (2.0–10.0), reaction time (5–40 min), initial adsorbent amount (1.0–7.0 mg), and sample volume (50–1000 mL) on the adsorption of Ni^{2+} ions was investigated. The temperature effect on the removal of Ni^{2+} ion was investigated in the range 5–50 °C. In a generic test, the 5 mg of nano Fe_3O_4/chitosan-acrylamide hydrogel and 50 mL of Ni^{2+} ions solution with 2 mg L^{-1} of concentration in the water sample was stirred at 25 °C for 40 min to get equilibrium mode (Moghimi, 2013). Afterward, the Ni^{2+} ions in the sample, in extraction by the Fe_3O_4/chitosan-acrylamide hydrogel, were determined by flame atomic absorption spectrophotometer using a calibration curve. In the case of the presence of interference in the aqueous samples, a certain variation of over ±5% was studied in the Ni^{2+} ions adsorption. Besides, all the models of isotherm studies were carried out at 25 °C. The capacity in

equilibrium sorption (q_e (mg g^{-1})) was obtained from the Eq. (1):

$$q_e = V(C_0 - C_e)/W \quad (1)$$

where C_e and C_0 are the equilibrium and initial Ni^{2+} ions concentration (mgL^{-1}) in each remaining solution, respectively. V term in Eq. 1 is the volume (L) of the Ni^{2+} ions sample and w (g) is sorbent mass (Salehi et al. 2022).

Desorption and recovery studies from the adsorbent

After the adsorption study, the Fe_3O_4/chitosan-acrylamide hydrogel loaded with Ni^{2+} ions was gathered and washed with multiple elution solvents (0.1–3 mol L^{-1} of HNO_3, 0.1 mol L^{-1} of HCl and 0.1 mol L^{-1} of NaOH). Also, the volume of optimum elution solvent (100–1000 mL) was investigated for Ni^{2+} ions recovery.

Reusability study of the nano Fe_3O_4/chitosan-acrylamide hydrogel

To check the nano Fe_3O_4/chitosan-acrylamide hydrogel reusability, the sorption-desorption experiments were performed 5 cycles repeatedly through specified processes. First, 50 mL of 0.2 mg L^{-1} solution of Ni^{2+} ions was prepared at pH = 6, and then 5 mg of nano Fe_3O_4/chitosan-acrylamide hydrogel was added and stirred for 15 min, then the sorbent was separated with a magnet and finally eluted with HNO_3 (2 M) and then the concentration of Ni^{2+} ions in solution was analyzed by FAAS. Then the adsorbent was eluted by water and ethanol and dried and re-examined for the second time according to the said method. This experiment was performed up to 5 times.

Check the repeatability of the method

To determine the repeatability of the method, first, 5 mg of nano Fe_3O_4/chitosan-acrylamide hydrogel was poured into 5 containers with 50 mL of 0.2 mg L^{-1} solution of Ni^{2+} ions and adjusted at pH = 6, then was stirred for 15 min and the sorbent was separated with a magnet and finally was eluted with 8 mL of HNO_3 (1 M). Finally, the solution was determined by flame atomic absorption spectroscopy.

Results and discussion

Characterizations

FTIR analysis

Figure 1a presents the findings of the FTIR investigation of the nano Fe_3O_4/chitosan-acrylamide hydrogel. The peak at 3442 cm^{-1} in the FTIR spectra is related to the OH. The peak at 3743 cm^{-1} is related to the H-bonding between NH_2 (Rahangdale & Kumar, 2018). The -CH stretch bond is related to the peaks at 2927 cm^{-1} and 2855 cm^{-1} (Jiang et al., 2015; Liu et al., 2021). Additionally, the stretching C=O vibration reached its peak at 1625 cm^{-1}. Bending vibration connected the Fe-O band in Fe_3O_4 to the peak at 525 cm^{-1} (Duru et al., 2016; Salehi et al., 2022). The N-H bond peak at 1457 cm^{-1} illustrates the amidation reaction between the carboxyl groups of polyacrylic acid and the amine groups of chitosan (Xiang et al., 2017). The FTIR spectra after Ni^{2+} ions adsorption is shown in Fig. 1b. When Ni^{2+} ions were adsorbed on the nano Fe_3O_4/chitosan-acrylamide hydrogel, the decrease in intensity of the absorption peak attributed to NH_2 and N-H at 3743 and 1457cm^{-1} proves that NH_2 and N-H may interact with Ni^{2+} ions.

X-ray diffraction analysis

Only two significant peaks, positioned at 8° and 21°, in the nano Fe_3O_4/chitosan-acrylamide hydrogel XRD pattern demonstrate acrylamide's amorphous nature. The presence of chitosan was shown by a peak at 2θ = 10° in Fig. 2(a) (Yuan et al., 2015). Peaks at 2θ = 35.5°, 57.15°, and 62.77°, respectively, correlate to magnetic particles and support the presence of Fe_3O_4 particles (Chen et al., 2014). The peak has emerged at 2θ =12° following the sorption of Ni^{2+} ions and may indicate the interaction between the amine group of chitosan and the Ni^{2+} ions (Fig. 2(b)).

SEM analysis

According to the SEM findings in Fig. 3a, the nano Fe_3O_4/chitosan-acrylamide hydrogel is made with nanometer particles that are placed on it and can be related to iron nanoparticles. Also, after the adsorption of Ni^{2+} ions by the nano Fe_3O_4/

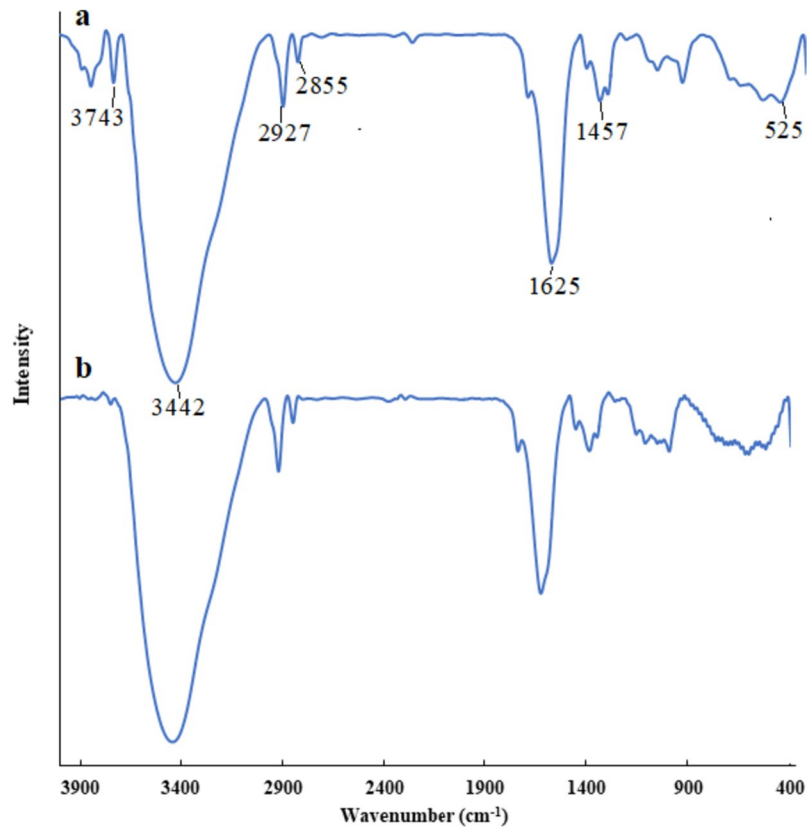

Fig. 1 FTIR spectra of nano Fe_3O_4/chitosan-acrylamide hydrogel **a** before Ni^{2+} ions adsorption and **b** after Ni^{2+} ions adsorption

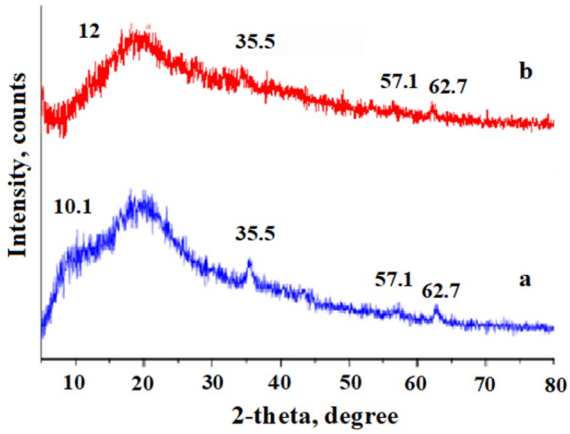

Fig. 2 XRD pattern of nano Fe_3O_4/chitosan-acrylamide hydrogel (a) before Ni^{2+} ions adsorption and (b) after Ni^{2+} ions adsorption

chitosan-acrylamide hydrogel, it can be seen that the morphology of the adsorbent has changed (Fig. 3b). The EDS analysis showed the constituent components of the adsorbent (Fig. 3c), and also the EDS represented the Ni^{2+} ion adsorption successfully by the nano Fe_3O_4/chitosan-acrylamide hydrogel (Fig. 3d).

Effective parameters on the adsorption of Ni^{2+} ions

pH optimization

The pH of Ni^{2+} ions solution affects the main feature of their adsorption by Fe_3O_4/chitosan-acrylamide nano hydrogel. In fact, the Ni^{2+} ions adsorption is associated mostly with the protonation and deprotonation of binding sites from ligand posited on the surface of nano Fe_3O_4/chitosan-acrylamide hydrogel (Salehi et al. 2022, Duran et al., 2008). The results obtained from pH changes in Ni^{2+} ions adsorption percentage showed that with the increase of solution pH to pH = 5, the Ni^{2+} adsorption percentage reached the maximum (Fig. 4). This is because at pHs below 4, nitrogen atoms of the ligand are protonated in an acidic environment and Ni^{2+} ions can be completely inhibited (Navarro et al., 2003). While at pH values

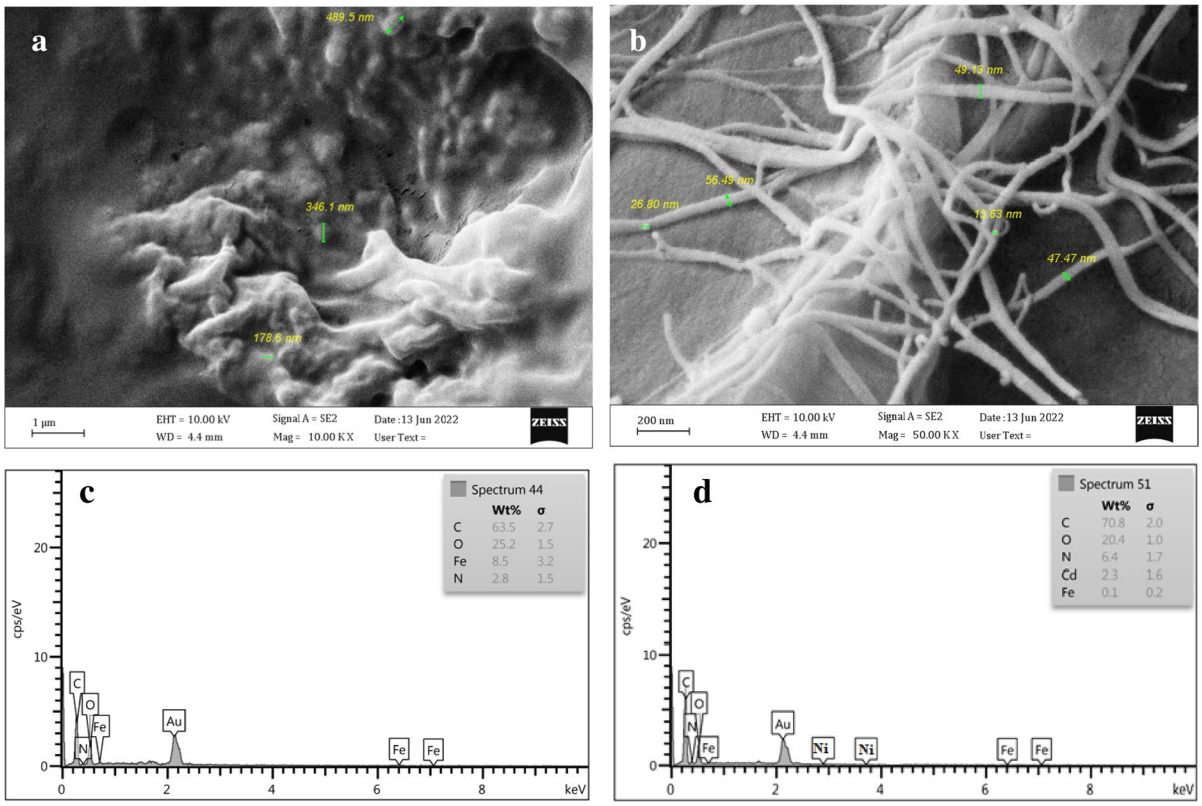

Fig. 3 **a** SEM image, **c** EDS analysis of nano Fe_3O_4/chitosan-acrylamide hydrogel before Ni^{2+} ions sorption, **b** SEM image, **d** EDS analysis of nano Fe_3O_4/chitosan-acrylamide hydrogel after Ni^{2+} ions sorption

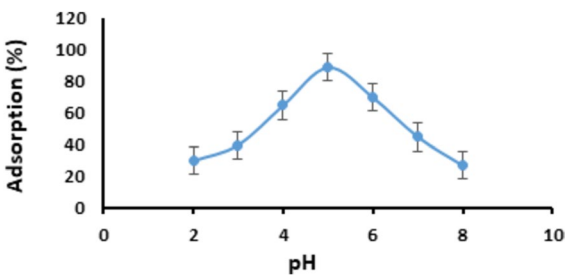

Fig. 4 The percentage of Ni^{2+} ions adsorption in terms of pH

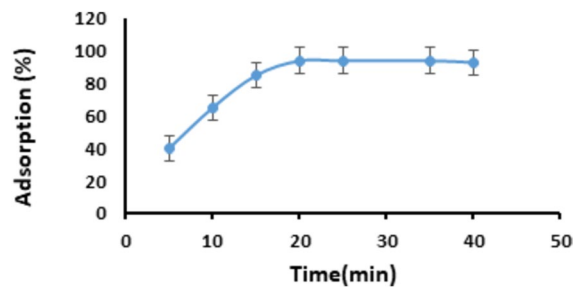

Fig. 5 Effect of contact time on the adsorption percentage of nano Fe_3O_4/chitosan-acrylamide hydrogel for Ni^{2+} ions

above 6, Ni^{2+} ions react with hydroxide ions to produce $Ni(OH)_2$.

Time effect

To know the sorption behaviors of nano Fe_3O_4/chitosan-acrylamide hydrogel towards Ni^{2+} spices, the adsorption percentage of Ni^{2+} ions at different contact times was investigated. The results of Fig. 5 showed that with the increased time to 20 min, the adsorption percentage increases because the Ni^{2+} ions in the solution have more opportunity to be adsorbed on the adsorbent functional groups.

Effect of adsorbent amount

The amount of nano Fe_3O_4/chitosan-acrylamide hydrogel has a great effect on adsorption. The results in Fig. 6 showed that by increasing the amount of nano Fe_3O_4/chitosan-acrylamide to 6 mg, the adsorption percentage increased and then the changes were insignificant, so 6 mg of nano Fe_3O_4/chitosan-acrylamide was chosen as the optimal adsorbent amount.

Temperature effect

According to the results in Fig. 7, the Ni^{2+} ions adsorption was changed in proportion to temperature, which is due to the changed diffusion rate and mobility of reactive species. The adsorption yield of Ni^{2+} ions onto nano Fe_3O_4/chitosan-acrylamide hydrogel was favorable at high temperatures because the mobility rate of reactive species was increased (Peer et al., 2018).

Sample volume effect

Figure 8 illustrates the effect of sample volume on Ni^{2+} ions adsorption by nano Fe_3O_4/chitosan-acrylamide hydrogel. The results indicated that the Ni^{2+} ions were adsorbed up to 200 mL of sample volume on the nano Fe_3O_4/chitosan-acrylamide hydrogel, after which the Ni^{2+} ions appeared in the sample solution. According to the definition of limit volume, the limit volume in this experiment is 200 mL, and if the volume of the sample solution containing Ni^{2+} ions is more than 200 mL, ions are not completely adsorbed.

Effect of interferences

An ion that causes more than a 5% change in the absorbance signal of the analyte is considered an interfering ion (Salehi et al., 2022). In the current research, the effect of ions interference was studied on Ni^{2+} ions adsorption by nano Fe_3O_4/chitosan-acrylamide hydrogel. According to the results

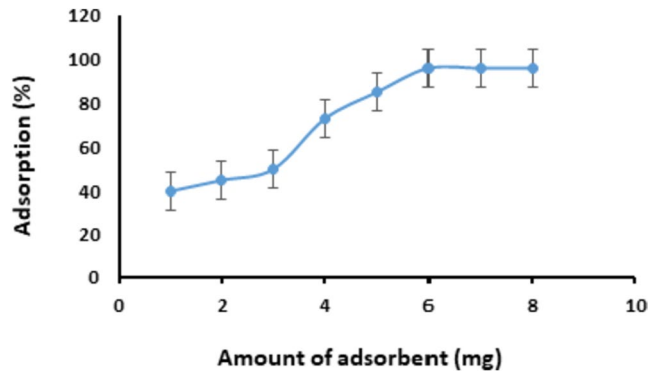

Fig. 6 Effect of nano Fe_3O_4/chitosan-acrylamide hydrogel amount on Ni^{2+} ions adsorption

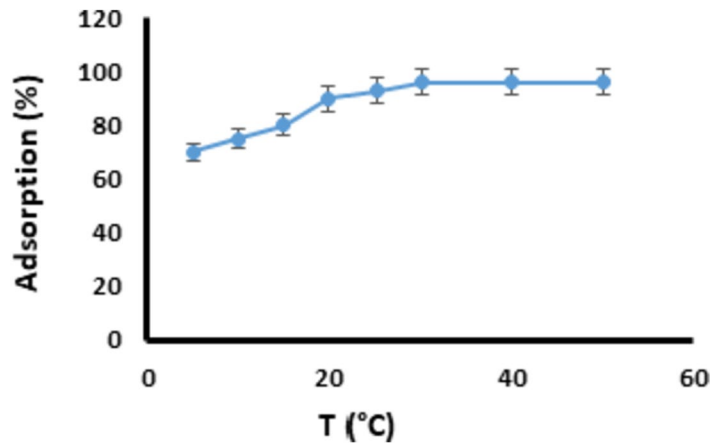

Fig. 7 Effect of temperature on Ni^{2+} ions adsorption

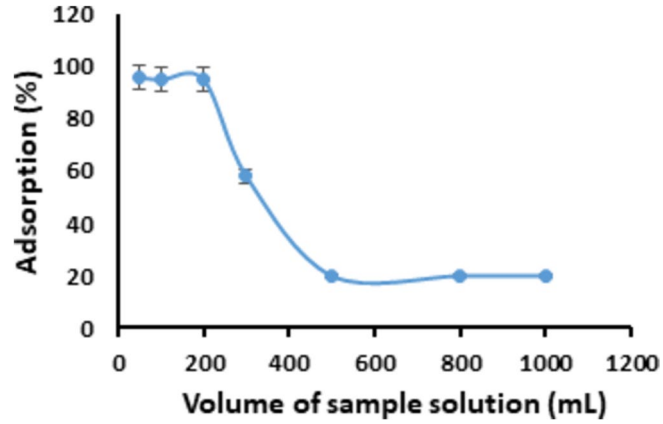

Fig. 8 Effect of sample solution volume on Ni^{2+} ions adsorption

Table 1 The adsorption percentage of Ni^{2+} ions in the presence of foreign ions

Interfering ion	$C_{metal\ ions}/C_{interfering\ ion}$	% recovery of Ni^{2+} ion
Na^+	100	98.3 (1.3)[a]
K^+	100	98.2 (1.2)
Ca^{2+}	100	99.8 (1.3)
Mg^{2+}	100	98.6 (1.4)
Fe^{2+}	100	98.8 (1.8)
Cr^{3+}	50	97.9 (1.2)
Co^{2+}	50	98.5 (1.8)
Cl^-	100	96.9 1.2)
Br^-	100	99.0 (1.0)
F^-	100	98.8 (1.9)
Mn^{2+}	100	99.8 (1.3)
Zn^{2+}	50	97.7 (0.5)

[a]Values in parentheses are % RSD based on three individual replicate analyses

showed in Table 1, the adsorption percentage of Ni^{2+} ions in the presence of foreign ions was well done, and foreign ions had little effect on the determination of Ni^{2+} ions.

Desorption

Effect of elution solvents on the recovery of Ni^{2+} ions

Among the parameters affecting the recovery system, the type of elution solvent is one of the main parameters that have a great impact on the recovery system. In this research, elution solvents including HNO_3, HCl, and NaOH were investigated to recover Ni^{2+} ions. Considering the maximum recovery for optimal solvent selection, the HNO_3 was selected for the extraction of Ni^{2+} ions from nano Fe_3O_4/chitosan-acrylamide hydrogel. The results reported in Fig. 9 demonstrated that in the balance created between the nano Fe_3O_4/chitosan-acrylamide hydrogel and the HNO_3 (1 M), more H^+ is replaced Ni^{2+} on the adsorbent and as a result, the more Ni^{2+} is extracted. The decrease in recovery at higher concentrations than 1 M can be due to molecular association between nitric acid molecules and a decrease in proton activity resulting in a decrease in the acidity of elution solvent. In this research, the volume of the HNO_3 (1 M) was investigated for Ni^{2+} ions recovery. Different volumes of HNO_3 (1 M) were

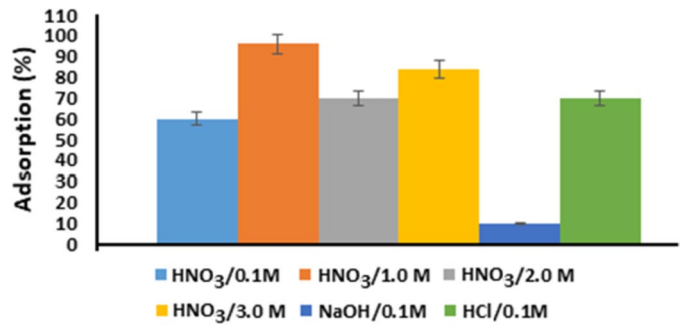

Fig. 9 Effect of elution solvent type on Ni^{2+} ions recovery

selected for Ni^{2+} ion extraction and the optimal volume of HNO_3 (1 M) was obtained at 6 mL. The results in Fig. 10 showed that from the volume of 6 mL onwards, all Ni^{2+} ions entered the solvent and the balance went slightly towards HNO_3 and recycling was complete. The concentration factor (33.3) was obtained as the ratio of the volume of the sample solution (200 mL) to the volume of the recovery solution (6 mL).

Stability and reusability evaluation

The cost of the adsorption system has a direct relationship with the potential for nano Fe_3O_4/chitosan-acrylamide hydrogel reusability. Therefore, the reusability and stability of the nano Fe_3O_4/chitosan-acrylamide hydrogel in the optimal condition of adsorption and desorption were investigated. The results showed that the nano Fe_3O_4/chitosan-acrylamide hydrogel can be reused more than 3 times without a profound loss of adsorption efficiency. After the first adsorbent recycling (adsorption and desorption), the nano Fe_3O_4/chitosan-acrylamide hydrogel retained about 90.2% of the adsorption efficiency retention for Ni^{2+} ions. Even after recycling the adsorbent 3 times, the adsorption efficiency of the nano Fe_3O_4/chitosan-acrylamide hydrogel was still 83.2% for Ni^{2+} ions (Fig. 11).

Adsorption mechanism

Because of the binding site (functional group) on modified chitosan, several mechanisms (dative band, coordination band, ion-exchange, etc.) can adsorbed Ni^{2+} ions on the adsorbent. In addition, according to the results about the pH of the sample solution, the dative and coordination bands probably occurred between the Ni^{2+} ions and the adsorbent (Salehi et al., 2020).

Adsorption isotherms

The survey of the isotherm models represents a good comprehension of the Ni^{2+} ions adsorption mechanism on nano Fe_3O_4/chitosan-acrylamide hydrogel. For this purpose, the models of Langmuir, Freundlich,

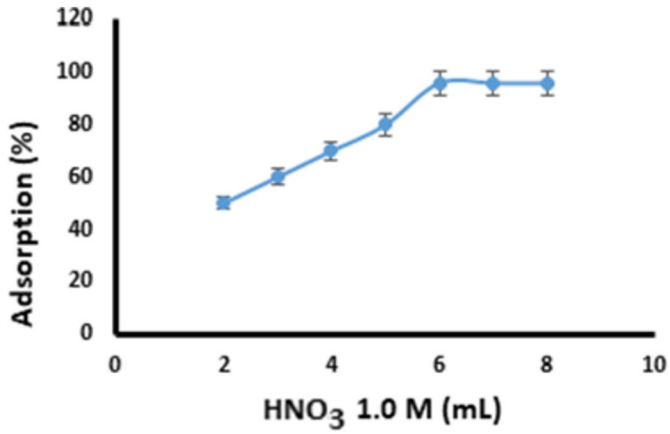

Fig. 10 Effect of elution solvent volume on Ni^{2+} ions recovery

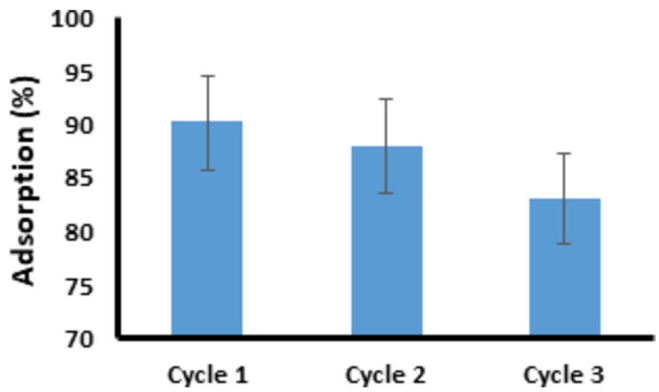

Fig. 11 Effect of elution solvent volume on Ni^{2+} ions recovery

and Temkin were used to fit the Ni^{2+} ion adsorption isotherms onto the nano Fe_3O_4/chitosan-acrylamide hydrogel. The isotherm of Langmuir is generally applied to qualify the sorption onto a uniform surface of adsorbent supposing the monotony of the sites of adsorption and not interplay among the analyte and adsorbent. The model in the linear form is expressed as (Kouotou et al., 2021):

$$C_e/q_e = \left(1/K_L q_{max}\right) + \left(C_e/q_{max}\right) \quad (2)$$

where, C_e (mgL^{-1}) is the concentration in the equilibrium of Ni^{2+} ions, q_e (mg g^{-1}) is the capacity of equilibrium adsorption, and q_m (mg g^{-1}) is the capacity of Langmuir monolayer saturation. The K_L (Lmg^{-1}) is a Langmuir constant related to the adsorption energy. This model can be expressed in other terms called separation coefficient (R_L) which is a dimensionless constant, giving data about the feasibility of the process of adsorption (Arvand et al., 2022, Salehi et al. 2022). It can be expressed as:

$$R_{L=}1/\left(1 + K_L C_0\right) \quad (3)$$

The Freundlich pattern is appropriate for explaining the adsorption enthalpy on an adsorbent with an uncoordinated surface, supposing the binding tendency reduces with the growth in the degree of adsorption. The linear term of this model is expressed as:

$$\ln\ q_e = \ln\ K_F\ +\ 1/n\left(\ln\ C_e\right) \quad (4)$$

The K_F and n terms are Freundlich constants and indicate the adsorption of capacity and intensity, respectively.

The Temkin model describes that the heat of adsorption with degree of surface coverage and uniform distribution of binding energies on the adsorbent surface decreases linearly and it can be expressed as:

$$q_e = \left(BlnK_T\right)\ +\ \left(Bln\ C_e\right) \quad (5)$$

The B and K_T are adsorption heat and maximum binding energy, respectively.

The isotherm models of Langmuir, Freundlich, and Temkin were applied to test the correlation among the Ni^{2+} ion sorption on nano Fe_3O_4/chitosan-acrylamide hydrogel. A parameter comparison among the two isotherms is shown in Table 2. As can be seen, the Langmuir model displayed a preferable value of correlation (R^2) and a premiere compatible with the empirical result than the model of the Freundlich, demonstrating that the Ni^{2+} ions adsorption onto nano Fe_3O_4/chitosan-acrylamide hydrogel was based on a unit layer and with chemisorption process on a monotonous surface. In addition, the R_L value was in the range of 0–1, which confirmed that the nano Fe_3O_4/chitosan-acrylamide hydrogel was the desired adsorbent of Ni^{2+} ions.

Adsorption kinetics of the Ni^{2+} ions

The kinetic result was analyzed with three used kinetic adsorption models, including the pseudo-first, second-order, and the Roginsky-Zeldovich models (Fig. 12). The pseudo-first-order model is written as follows:

$$1/q_t = \left(K_1/q_e t\right) + \left(1/q_e\right) \quad (6)$$

In Eq. 5, q_e and q_t terms (mg g^{-1}) are the adsorption value in equilibrium and t (min), respectively; K_1 (min^{-1}) is the pseudo-first-order rate constant. The linear model of the pseudo-second-order pattern could be displayed as follows:

$$t/q_t = \left(1/K_2 q_e^2\right) + \left(t/q_e\right) \quad (7)$$

In Eq. 7, K_2 (g (mg min)$^{-1}$) is the constant of the pseudo-second-order rate.

The linear form of the Roginsky-Zeldovich model is given as:

$$q_t = \frac{1}{\beta}\log\left(\alpha \times \beta\right) + \frac{1}{\beta}\log t \quad (8)$$

Table 2 Langmuir, Freundlich, and Temkin isotherm parameters for Ni^{2+} ions adsorption

Isotherm models									
Langmuir				Freundlich			Temkin		
q_{max} (mg g^{-1})	K_L (L mg^{-1})	R_L	R^2	n	K_F (mg g^{-1}) (mg $L^{-1})^{-n}$	R^2	R^2	B (L g^{-1})	K_T
172.4	0.0261	0.2098	0.9911	2.71	20.57	0.9723	0.9626	2.98	2.02

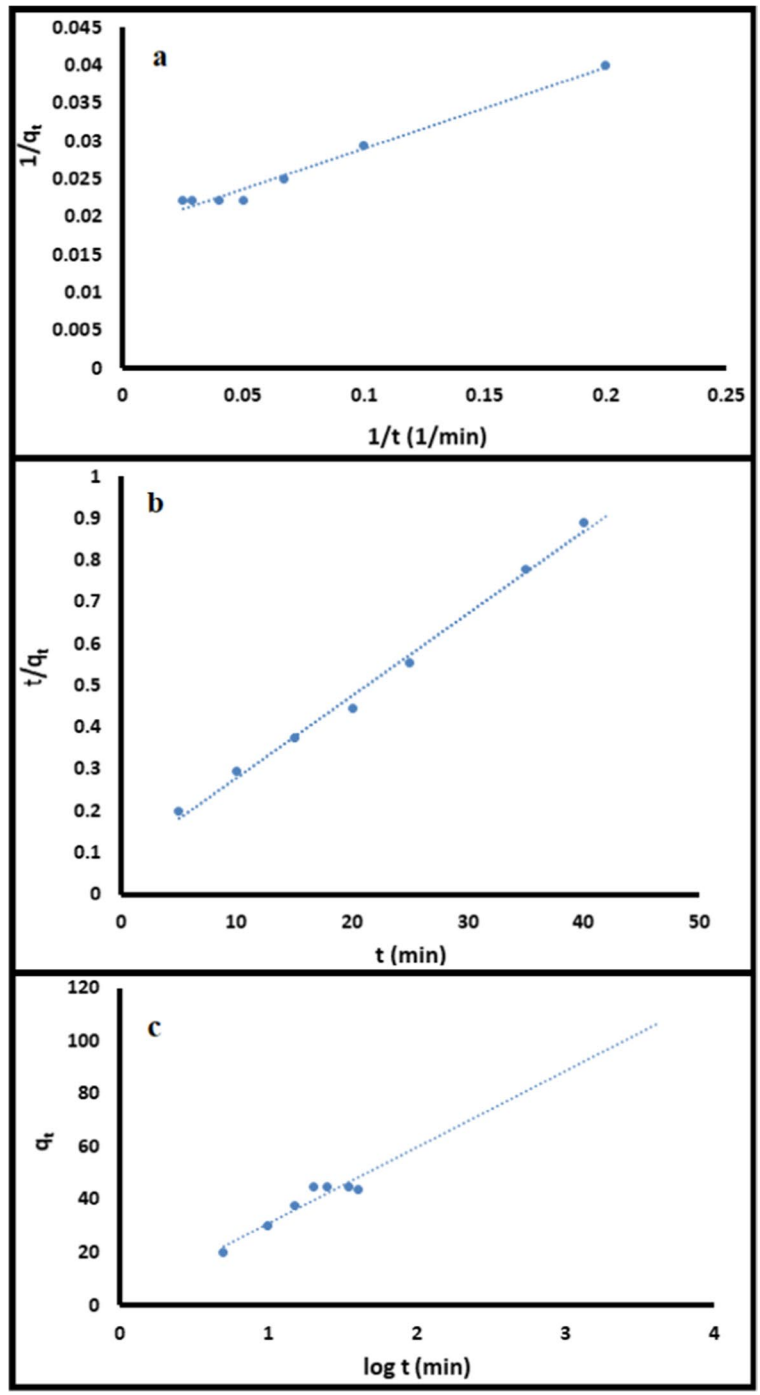

Fig. 12 The pseudo-first-order model (**a**), pseudo-second-order model (**b**), and Roginsky-Zeldovich model (**c**) of Ni^{2+} ions adsorption kinetics

where α (mg (g min)$^{-1}$) is the rate of Roginsky-Zeldovich initial sorption. (g mg^{-1}) is a constant of desorption (Kanmaz et al., 2020).

According to R^2 in Table 3, the pseudo-second-order model was fitted with a better kinetic result than the pseudo-first-order adsorption model. The Roginsky-Zeldovich model was vastly applied to qualify the pseudo-second-order model and was remarked that the nano Fe_3O_4/chitosan-acrylamide hydrogel surface was uncoordinated. The kinetic constant values of

the Roginsky-Zeldovich equation for Ni^{2+} ions were deposited in Table 3. According to the R^2 value, it could be derived that the Roginsky-Zeldovich model is well adapted to explain the Ni^{2+} ions sorption onto the Nano Fe_3O_4/chitosan-acrylamide hydrogel compared with a model of the pseudo-first-order.

Thermodynamics study for adsorption of Ni^{2+} on nano Fe_3O_4/chitosan-acrylamide hydrogel

Thermodynamic parameters for the adsorption of Ni^{2+} on nano Fe_3O_4/chitosan-acrylamide hydrogel are reported in Table 4. The values of ΔG were reported negative which indicated the process of adsorption to be favorable and spontaneous. With increasing temperature, the negative values of ΔG decrease, indicating that the adsorption process is less spontaneous and exothermic. Also, negative values for ΔS indicate random reduction at the solid-solution interface of nano Fe_3O_4/chitosan-acrylamide hydrogel. Negative values of ΔH is −24.45 (KJ mol^{-1}) were obtained, which shows physical adsorption and chemical adsorption occur in the adsorption process (Joshi & Srivastava, 2019).

Analytical performance

Precisions of method

The precisions of this method was obtained from relative standard deviation (RSD) and by measuring the Ni^{2+} ions adsorption of 5 solutions in intra- and inter-day. To do this, 5 standard solutions of Ni^{2+} ions with the optimal conditions were prepared (Ashrafzadeh & Qomi, 2016). By obtaining the maximum adsorption of Ni^{2+} ions, the RSD based on intra-day and inter-day was achieved in 1.80% and 0.95% ($n = 3$), respectively.

Repeatability of the method

The reproducibility of each method is an important factor in determining reliability. Based on the results, 1.8% was obtained for reproducibility.

Application on real samples

After the dispersive extraction technique was completed with nano Fe_3O_4/chitosan-acrylamide hydrogel and optimal conditions were found for it, several real samples of water and wastewater were analyzed. The real samples included the Varamin tap water, Tehran tap water, synthetic samples, Charshahr factory effluent, and Shahre Rey University effluent. These water samples were collected with 10 suitable PET bottles for each sample. The bottles were washed with plain water and a suitable detergent solution. Then they were filled with a nitric acid solution (1 M) and were left overnight. The bottles were then washed with plain and distilled water and after that, the bottles were completely dried and labeled. The colloidal and suspended particles were removed with filtration, then their pH was adjusted to 5 for each sample. For the first time, the water samples were injected into the device without any concentration and separation. In the second time, increasing the concentration of Ni^{2+} ions and separating them was done according to the presented method, and then water samples were injected into the device. The results of this analysis are shown in Table 5. As can

Table 3 Estimated parameters of adsorption kinetics for the adsorption of Ni^{2+} ions on nano Fe_3O_4/chitosan-acrylamide hydrogel

Pseudo-first order		Pseudo-second order		Roginsky-Zeldovich	
q_e (mg g^{-1})	0.68	q_e (mg g^{-1})	4.39	α (mg (g min)$^{-1}$)	6.76
k_1 (min^{-1})	0.09	k_2 (g (mg min)$^{-1}$)	0.003	β (g mg^{-1})	1.48
R^2	0.9817	R^2	0.9938	R^2	0.8838

Table 4 Thermodynamic parameters for adsorption of Ni^{2+} on nano Fe_3O_4/chitosan-acrylamide hydrogel

Temperature (Kelvin)	Kc	ΔG° (KJ mol^{-1})	ΔH° (KJ mol^{-1})	ΔS° (J(mol K) $^{-1}$)	R^2
303.15 (30 °C)	4.07	−3.49	−24.45	−65.24	93.59
313.15 (40 °C)	2.75	−2.69			
323.15 (50 °C)	2.05	−1.68			
333.15 (60 °C)	1.98	−0.85			

Table 5 Determination of Ni^{2+} ions in real samples

Samples	Added Ni (II) (μg))	Atomic absorption (flame)	Atomic absorption (furnace)
Tehran tap water	0	N.D[a]	N.D
	10.00	10.07 (1.3)[b]	10.06 (2.4)
Varamin tap water	0	5.04 (1.4)	5.19 (2.3)
	10.00	15.65 (1.6)	15.46 (2.5)
Charshahr factory effluent	0	67.06 (2.0)	66.31 (2.9)
	10	77.09 (1.7)	75.89 (2.2)
Varamin university effluent	0	20.03 (1.3)	19.87 (2.5)
	10.00	30.06 (2.0)	29.90 (2.3)
Synthetic samples (Co^{2+}, Pb^{2+}, Na^{+}, Al^{3+}, Ba^{2+}, Ca^{2+}, Cu^{2+}) 0.02 mg	0	N.D	N.D
	10.00	10.66 (2.1)	10.40 (1.7)

[a]Not detected

[b]Values in parentheses are % RSD based on three individual replicate analyses

be seen, there are more Ni^{2+} ions in the sample of the Charmshahr factory effluent and Varamin University effluent, respectively, but there were no Ni^{2+} ions in the tap water sample. There is also a small amount of Ni^{2+} ions in the water sample of the Varamin. The proposed method has been able to detect the trace amount of Ni^{2+} ions in the synthetic sample without observing a large difference in the amount of Ni^{2+} ions.

Paired t-test

The *T* test was used to compare the value obtained from the furnace atomic absorption method with graphite atomic spectroscopy. Following the values obtained for *T* and the test results, it was observed that with a 95% confidence interval, there is no significant difference between the values obtained by the atomic absorption method of the flame atomic absorption furnace. Therefore these two methods can be used for the determination of Ni^{2+} ions in water samples.

Comparison of the removal of Ni^{2+} ions by various adsorbents and methods

Table 6 showed some parameters such as concentration factor and relative standard deviation of Ni^{2+} ions by for various adsorbents and methods. Results demonstrated the proposed method is more accurate,

Table 6 Comparison of the removal of Ni^{2+} ions by various adsorbents and methods

Method	Adsorbent type	Amount of adsorbent (milligrams)	Concentration factor	Relative standard deviation	Ref
On-line solvent extraction–GF AAS	Ammonium diethyl dithiophosphate	14.0	24.6	3.2	Anthemidis et al., 2003
CO-Precipitation–GF AAS	Ytterbium hydroxide	25.0	100	3.2	Atsumi et al., 2005
On-line SPE–GF AAS	Diethyldithiophosphate	3	59.4	1.3	Wang & Hansen, 2002
CPE-GF AAS	P-octyl polyethyleneglycol-phenyether	10.0	50	2.1	Zhu et al., 2006
SDME-GF AAS	Dithizone–chloroform	5.0	65	7.4	Fan & Zhou, 2006
SPE	Nano Fe_3O_4/chitosan-acrylamide hydrogel	5.0	33.3	1.8	This work

simpler, and faster because it has less relative standard deviation [31-35] (Anthemidis et al., 2003 ; Atsumi et al., 2005 ; Fan & Zhou, 2006 ; Wang & Hansen, 2002 ; Zhu et al., 2006).

Conclusion

The current research was to promote an efficient, easy, inexpensive, and selectable method for the removal of Ni^{2+} ions in several samples of water and wastewater. For the synthesis of a new Fe_3O_4/chitosan-acrylamide hydrogel, a multistep modification method was applied to the sorbent surface. However, the recovery of Ni^{2+} ions was studied and it was displayed the pH of the samples, the time of contact, and the temperature notably affect its recovery. Besides, it was displayed that the nano Fe_3O_4/chitosan-acrylamide hydrogel exhibits the high ability to adsorb Ni^{2+} ions (the capacity in equilibrium sorption = 22.54 mg g^{-1}) at pH = 5. The Langmuir isotherm was the most convenient one to explain the sorption of Ni^{2+} ions by the nano Fe_3O_4/chitosan-acrylamide hydrogel. Among the different washing solvents, the HNO_3 (1 M) demonstrated the best Ni^{2+} ions recovery. Then, the pseudo-second-order kinetic model was the most proper one to describe the adsorption of Ni^{2+} ions by the nano Fe_3O_4/chitosan-acrylamide hydrogel. The value of change in entropy (ΔS) obtained is −65.24 (J(mol K)$^{-1}$). Negative values of change in enthalpy, ΔH in is −24.45 (kJ mol^{-1}) which indicates both physical and chemical adsorptions involved in the process of adsorption. Finally, the resulting dispersive solid-phase extraction based on nano Fe_3O_4/chitosan-acrylamide hydrogel adsorbent presented a high extraction efficiency of Ni^{2+} ions from various water and wastewater samples.

Author contribution Morteza Parsayi Arvand performed the analysis. Ali Moghimi supervised the analyses and he is the corresponding author. Narges Salehi Performed the analysis and wrote the main manuscript text. All authors reviewed the manuscript.

Data availability All of the data and material are owned by the authors and/or no permissions are required. All authors (Morteza Parsayi Arvand, Ali Moghimi, and Narges Salehi) have read, understood, and have complied as applicable with the statement on "Ethical responsibilities of Authors" as found in the Instructions for Authors and are aware that with minor exceptions, no changes can be made to authorship once the paper is submitted.

Declarations

Conflicts of interest The authors declare they have no financial interests.

References

Al-Karawi, A. J. M., Al-Qaisi, Z. H. J., Abdullah, H. I., & Al-Mokaram, A. M. A. (2011). Al-Heetimi, D.T.A. Synthesis, characterization of acrylamide grafted chitosan and its use in removal of copper(II) ions from water. *Carbohydrate Polymers, 83*, 495–500. https://doi.org/10.1016/J.CARBPOL.2010.08.017

Anthemidis, A. N., Zachariadis, G. A., & Stratis, J. A. (2003). Development of an on-line solvent extraction system for electrothermal atomic absorption spectrometry utilizing a new gravitational phase separator. Determination of cadmium in natural waters and urine samples. *Journal of Analytical Atomic Spectrometry, 18*, 1400–1403. https://doi.org/10.1039/b308325j

Arvand, M. P., Moghimi, A., & Abniki, M. (2022). Extraction of alprazolam in biological samples using the dispersive solid-phase method with nanographene oxide grafted with α-pyridylamine. *IET Nanobiotechnology*. https://doi.org/10.1049/nbt2.12105

Ashrafzadeh, T., & Qomi, M. (2016). Preconcentration and determination of solifenacin using hollow fiber microextraction coupled with HPLC. *Current Analytical Chemistry, 12*, 594–601. https://doi.org/10.2174/1573411012666160606170219

Atsumi, K., Minami, T., & Ueda, J. (2005). Determination of cadmium in spring water by graphite-furnace atomic absorption spectrometry after coprecipitation with ytterbium hydroxide. *Analytical Sciences, 21*, 647–649. https://doi.org/10.2116/analsci.21.647

Bagheri, H., Zandi, O., & Aghakhani, A. (2011). Extraction of fluoxetine from aquatic and urine samples using sodium dodecyl sulfate-coated iron oxide magnetic nanoparticles followed by spectrofluorimetric determination. *Analytica Chimica Acta, 692*, 80–84. https://doi.org/10.1016/j.aca.2011.02.060

Boudreau, S. P., & Cooper, W. T. (1989). Analysis of thermally and chemically modified silica gels by heterogeneous gas-solid chromatography and infrared spectroscopy. *Analytical Chemistry, 61*, 41–47. https://doi.org/10.1021/ac00176a010

Chen, Y., He, M., Wang, C., & Wei, Y. (2014). A novel polyvinyltetrazole-grafted resin with high capacity for adsorption of Pb (II), Cu (II) and Cr (III) ions from aqueous solutions. *Journal of Materials Chemistry A, 2*, 10444–10453. https://doi.org/10.1039/c4ta01512f

Duran, A., Soylak, M., & Tuncel, S. A. (2008). Poly (vinyl pyridine-poly ethylene glycol methacrylate-ethylene glycol dimethacrylate) beads for heavy metal removal. *Journal of Hazardous Materials, 155*, 114–120. https://doi.org/10.1016/j.jhazmat.2007.11.037

Duru, İ., Ege, D., & Kamali, A. R. (2016). Graphene oxides for removal of heavy and precious metals from wastewater. *Journal of Materials Science, 51*, 6097–6116. https://doi.org/10.1007/s10853-016-9913-8

Fan, Z., & Zhou, W. (2006). Dithizone–chloroform single drop microextraction system combined with electrothermal atomic absorption spectrometry using Ir as permanent modifier for the determination of Cd in water and biological samples. *Spectrochimica Acta Part B: Atomic Spectroscopy, 61*, 870874. https://doi.org/10.1016/j.sab.2006.05.011

Fu, F. L., & Wang, Q. (2011). Removal of heavy metal ions from wastewaters: A review. *Journal of Environmental Management, 92*, 407–418. https://doi.org/10.1016/j.jenvman.2010.11.011

Ghazanfar, S., Komal, A., Waseem, A., Hassan, W., Iqbal, I. J., Toor, S., Asif, M., Saleem, I. A., Khan, S. U., Tarar, Z. H., Nazar, S., Rehman, H. U., Ahmed, M. I., & Rebi, A. (2021). Physiological effects of nickel contamination on plant growth. *Natural Volatiles & Essential Oils, 8*, 13457–13469.

Gomes-Gomes, M. M., Hidalgo Garcia, M. M., & Palacio Corvillo, M. A. (1995). On-line preconcentration of silver on a sulfhydryl cotton microcolumn and determination by flow injection atomic absorption spectrometry. *Analyst, 120*, 1911–2915. https://doi.org/10.1039/AN9952001911

Izatt, R. M., Bradshaw, J. S., Nielsen, S. A., Lamb, J. D., Christensen, J. J., & Sen, D. (1985). Thermodynamic and kinetic data for cation-macrocycle interaction. *Chemical Reviews, **85***, 271–399. https://doi.org/10.1021/cr00068a003

Jiang, T., Liu, W., Mao, Y., Zhang, L., Cheng, J., Gong, M., Zhao, H., Dai L., Zhang S., Zhao Q. (2015). Adsorption behavior of copper ions from aqueous solution onto graphene oxide–CdS composite. *Chemical Engineering Journal*, 259, 603-610. https://doi.org/10.1016/j.cej.2014.08.022

Joshi, S., & Srivastava, R. K. (2019). Adsorptive removal of lead (Pb), copper (Cu), nickel (Ni) and mercury (Hg) ions from water using chitosan silica gel composite. *Environmental Monitoring and Assessment, 191*, 615. https://doi.org/10.1007/s10661-019-7777-5

Kanmaz, N., Acar, M., Yılmazoğlu, M., & Hızal, J. (2020). Rhodamine B and murexide retention onto sulfonated poly (ether ether ketone) (sPEEK). *Colloids and Surfaces A: Physicochemical and Engineering Aspects, 605*, 125341. https://doi.org/10.1016/j.colsurfa.2020.125341

Khan, A., Badshah, S., & Airoldi, C. C. (2011). Biosorption of some toxic metal ions by chitosan modified with glycidylmethacrylate and diethylenetriamine. *Chemical Engineering Journal, 171*, 159–166. https://doi.org/10.1016/j.cej.2011.03.081

Kouotou, D., Ghalit, M., Ndi, J. N., Martinez, L. M. P., Ouahabi, M. E., Ketcha, J. M., & Gharibi, E. K. (2021). Removal of metallic trace elements (Pb2+, Cd2+, Cu2+, and Ni2+) from aqueous solution by adsorption onto cerium oxide modified activated carbon. *Environmental Monitoring and Assessment, 193*, 467. https://doi.org/10.1007/s10661-021-09267-9

Kvitek, R. J., Evans, J. F., & Carr, P. W. (1982). Diamine/silane-modified controlled pore glass: The covalent attachment reaction from aqueous solution and the mechanism of reaction of bound diamine with copper(II). *Analytica Chimica Acta, 144*, 93–106. https://doi.org/10.1016/S0003-2670(01)95522-9

Liu, X., Ma, R., Zhuang, L., Hu, B., Chen, J., Liu, X., Wang,X. (2021). Recent developments of doped g-C_3N_4 photocatalysts for the degradation of organic pollutants. *Critical Reviews in Environmental Science and Technology*, 51, 751-790. https://doi.org/10.1080/10643389.2020.1734433

Miretzky, P., Cirelli, A.F. (2009). Hg (II) removal from water by chitosan and chitosan derivatives. A review, *Journal of Hazardous Materials* 167, 10–23. https://doi.org/10.1016/j.jhazmat.2009.01.060

Moghimi, A. (2013). Detection of trace amounts of Pb (II) by schiff base-chitosan-grafted multiwalled carbon nanotubes. *Russian Journal of Physical Chemistry A, 87*, 1203–1209. https://doi.org/10.1134/s0036024413070388

Mourya, V. K., & Inamdar, N. N. (2008). Chitosan-modifications and applications : Opportunities galore. *Reactive and Functional polymers, 68*, 1013–1051. https://doi.org/10.1016/j.reactfunctpolym.2008.03.002

Navarro, R., Guzmán, J., Saucedo, I., Revilla, J., & Guibal, E. (2003). Recovery of metal ions by chitosan: Sorption mechanisms and influence of metal speciation. *Macromolecular Bioscience, 3*, 552–561. https://doi.org/10.1002/mabi.200300013

Peer, F. E., Bahramifar, N., & Younesi, H. (2018). Removal of Cd (II), Pb (II) and Cu (II) ions from aqueous solution by polyamidoamine dendrimer grafted magnetic graphene oxide nanosheets. *Journal of the Taiwan Institute of Chemical Engineers, 87*, 225–240. https://doi.org/10.1016/j.jtice.2018.03.039

Rahangdale, D., & Kumar, A. (2018). Acrylamide grafted chitosan based ion imprinted polymer for the recovery of cadmium from Nickel -Cadmium battery waste. *Journal of Environmental Chemical Engineering, 6*, 1828–1839. https://doi.org/10.1016/j.jece.2018.02.027

Rasoulzadeh, H., Sheikhmohammadi, A., Abtahi, M., Roshan, B., & Jokar, R. (2021). Eco-friendly rapid removal of palladium from aqueous solutions using alginate-diatomite magnano composite. *Journal of Environmental Chemical Engineering, 9*, 105954. https://doi.org/10.1016/j.jece.2021.105954

Sadeghi-Kiakhani, M., Safapour, S., & Ghanbari-Adivi, F. (2019). Grafting of chitosan-acrylamide hybrid on the wool: Characterization, reactive dyeing, antioxidant and antibacterial studies. *International Journal of Biological Macromolecules, 134*, 1170–1178. https://doi.org/10.1016/j.ijbiomac.2019.05.144

Salehi, N., Moghimi, A., & Shahbazi, H. (2020). Preparation of cross-linked magnetic chitosan with methionine-glutaraldehyde for removal of heavy metals from aqueous solutions. *International Journal of Environmental Analytical Chemistry, 102*, 2305–2321. https://doi.org/10.1080/03067319.2020.1753718

Salehi, N., Moghimi, A., & Shahbazi, H. (2022). Magnetic nanobiosorbent (MG-Chi/Fe_3O_4) for dispersive solid-phase extraction of Cu(II), Pb(II), and Cd(II) followed by flame atomic absorption spectrometry determination, *IET. Nanobiotechnology, 15*, 575–584. https://doi.org/10.1049/nbt2.12025

Varma, A. J., Deshpande, S. V., & Kennedy, J. F. (2004). Metal complexation by chitosan and its derivatives : a review. *Carbohydrate Polymers, 55*, 77–93. https://doi.org/10.1016/j.carbpol.2003.08.005

Wang, J., & Hansen, E. H. (2002). Sequential injection on-line matrix removal and trace metal preconcentration using a PTFE beads packed column as demonstrated for the determination of cadmium by electrothermal atomic absorption spectrometry. *Journal of Analytical Atomic Spectrometry, 17*, 248–252. https://doi.org/10.1039/b111089f

Wierucka, M., & Biziuk, M. (2014). Application of magnetic nanoparticles for magnetic solid-phase extraction in preparing biological, environmental and food samples. *TrAC Trends in Analytical Chemistry, 59*, 50–58. https://doi.org/10.1016/j.trac.2014.04.007

Xiang, B., Ling, D., Lou, H., & Gu, H. (2017). 3D hierarchical flower-like nickel ferrite/manganese dioxide toward lead (II) removal from aqueous water. *Journal of Hazardous Materials, 325*, 178–188. https://doi.org/10.1016/j.jhazmat.2016.11.011

Yuan, S., Gu, J., Zheng, Y., Jiang, W., Liang, B., & Pehkonen, S. O. (2015). Purification of phenol-contaminated water by adsorption with quaternized poly (dimethylaminopropyl methacrylamide)-grafted PVBC microspheres. *Journal of Materials Chemistry A, 3*, 4620–4636. https://doi.org/10.1039/c4ta06363e

Zhu, X., Zhu, X., & Wang, B. (2006). Determination of trace cadmium in water samples by graphite furnace atomic absorption spectrometry after cloud point extraction. *Microchimica Acta, 154*, 95–100. https://doi.org/10.1007/s00604-005-0476-7